

## The Application of Mineral Phase Diagrams to Geothermal Corrosion

W.F. Giggenbach

Chemistry Division, DSIR, Petone, New Zealand

Abstract - The thermodynamic stability of iron oxide and sulfide phases in contact with geothermal steam is presented in terms of  $P_{H_2} - \log \frac{Fe^{2+}}{(H^+)^2}$  - diagrams. For Wairakei high pressure steam lines (180°C), the mineralogy of the corrosion products (magnetite-pyrite) observed corresponds closely to that expected from theory. The overall corrosion process consists in the cyclic dissolution of metallic iron on contact with liquid condensate formed through heat loss from the pipe walls, subsequent increases in pH,  $P_{H_2}$  and iron contents of the condensate lead to the deposition of magnetite and later on pyrite until equilibrium between scale deposit, condensate and steam is reached. Continuing formation of fresh condensate, however, leads to undersaturation with respect to the scale deposit and to the dissolution of the protective layer of magnetite further downstream until bare metal is exposed again and the cycle is repeated. For Kawerau and Broadlands, higher  $H_2S$  partial pressures are predicted to lead to the exclusive formation of iron-sulfides (pyrrhotite-pyrite). Techniques to control pipeline corrosion include suppression of condensate formation through superheating of the steam carried and the addition of aluminium and silica through injection of separated thermal water or the slow leaching of cement or concrete surfaces in contact with the condensate to promote the formation of a protective iron-aluminium-silicate scale.

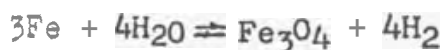
## Introduction

'After about 15 years of service the effects of corrosion on steam pipelines at Wairakei have become serious. On average the corrosion pits formed over the lower half of the inner circumference of the pipes are around 2-3 mm deep but in places reach a depth of 6 mm at a wall thickness of 13 mm. (Page, 1978). The main corrosion product is magnetite' forming well crystallised deposits of up to 3 mm thick. The distribution, geometry, and appearance of the corrosion patches has been described by Braithwaite (1979) who also carried out a detailed micrographic study of the deposits. He ascribes the corrosion to attack by the condensate film accumulating over the lower parts of the pipes. (Corrosion products (magnetite) are deposited downstream of the quite regularly distributed corrosion patches, he suggests that corrosion has been in progress for at least 10 years.

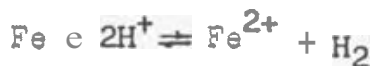
In order to get a better understanding of the corrosion process, electrochemical phase diagrams (Pourbaix, 1949) have been presented (Pound, Sharp and Wright, 1979). These  $E_h$  - pH-diagrams, however, can only be constructed by fixing the usually unknown activities of dissolved iron and sulfur species at more or less arbitrary levels. In this study an attempt is made to represent thermodynamic data in terms of readily determined parameters, such as hydrogen and hydrogen sulfide partial pressures, with no need to fix iron activities or pH.

## Thermodynamic Relationships

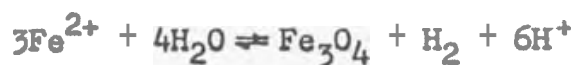
The chemical system underlying the corrosion processes at Wairakei is relatively simple. Steam, containing carbon dioxide, hydrogen sulfide, ammonia, hydrogen, methane and a series of other trace constituents (He, Ar, N<sub>2</sub>, and higher hydrocarbons) moves through pipes consisting of close to pure iron. Due to some heat loss from the pipes, small amounts of condensate form which in turn attack the pipes leading to dissolution of iron and subsequent deposition of magnetite according to the overall reaction.



This overall reaction can be broken down into several specific reactions taking place e.g. on the exposed iron surface



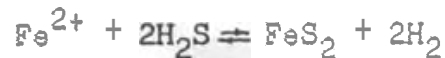
or during the deposition of magnetite



In the presence of hydrogen sulfide, we also have to consider possible formation of iron sulfide minerals such as pyrrhotite



or pyrite



A chemical model of the pipeline-geothermal system, therefore, should include the following constituents



Of these the activities of the solid mineral phases can be taken to be unity, those of the gases can be equated to their partial pressures, leaving the activity of  $\text{Fe}^{2+}$  and pH. These latter two parameters may be combined to form the new reaction parameter  $R = \log (\text{Fe}^{2+} / (\text{H}^+)^2)$ . By using  $P_{\text{H}_2}$  and  $R$  as coordinates, the thermodynamic stability of the iron phases can be expressed in terms of an analytically accessible parameter,  $P_{\text{H}_2}$ , and one,  $R$ , fully determined by thermodynamic relationships as shown in Figure 1 for a system at 180°C.

The equilibrium constants required to construct the stability diagram were calculated by use of SUPCRT (Helgeson et al., 1978), a computer program incorporating a critically evaluated set of internally consistent thermodynamic data.

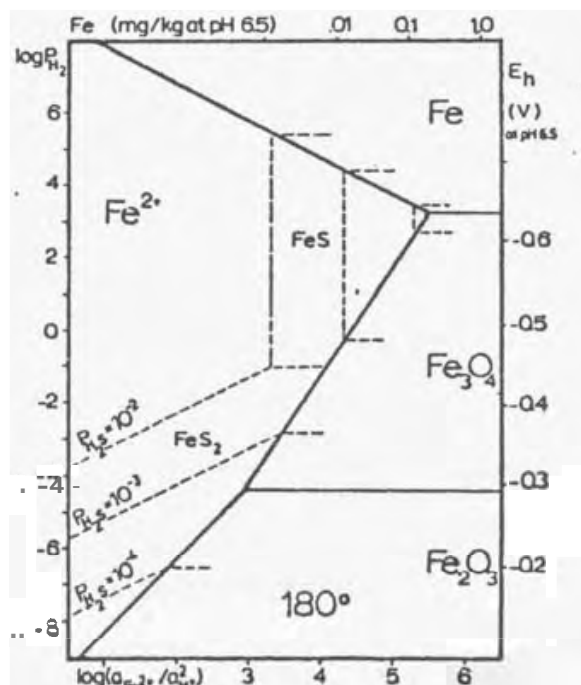


Figure 1 - The stability of iron species in contact with geothermal steam at 180° as a function of  $P_{\text{H}_2}$ ,  $P_{\text{H}_2\text{S}}$  and the ratio  $a_{\text{Fe}^{2+}} / a_{\text{H}^+}^2$ .

In constructing the diagram, the stability areas for  $\text{Fe}^{2+}$ ,  $\text{Fe}$ ,  $\text{Fe}_3\text{O}_4$  and  $\text{Fe}_2\text{O}_3$  were first determined for  $\text{H}_2\text{S}$  - free steam at a temperature of around  $180^\circ$  and a pressure of 10 bar, typical for high pressure Wairakei pipelines. Addition of  $\text{H}_2\text{S}$  to the system at partial pressures above  $10^{-4}$  bar leads to the appearance of a stability field for pyrrhotite replacing the iron-magnetite boundary and increasing with increasing  $\text{P}_{\text{H}_2\text{S}}$ . The stability field for pyrite also moves into the  $\text{Fe}^{2+}$  field with increasing  $\text{P}_{\text{H}_2\text{S}}$  and merges with the pyrrhotite field at  $\text{P}_{\text{H}_2\text{S}} > 10^{-3.5}$  bar. The formation of siderite,  $\text{FeCO}_3$ , competes with that of pyrrhotite and pyrite but is restricted to  $\text{CO}_2 / \text{H}_2\text{S}$  - ratios  $> 1700$ .

### The Composition of Steam Produced from New Zealand

#### Geothermal Areas

The composition of steam carried in Wairakei, Kawerau and Ohaki steam lines is given in Table 1. For Kawerau and Broadlands analyses of three well discharges separated under close to production conditions and considered representative of the geothermal field are given. Total gas contents for Kawerau and Broadlands are at around 1% quite uniform and considerably higher than those at Wairakei with ~.06%. On the other hand relative  $\text{H}_2\text{S}$  contents vary from around 50 mmol/mol at Wairakei over 35 at Kawerau to around 14 mmol/mol at Broadlands. Gas partial pressures in the pipelines may be calculated from these analyses by use of the relationship

$$P_1 = P_t x_g x_i / 10^6 \quad (\text{bar})$$

where  $P_t$  and  $P_1$  are total steam pressure and partial pressure of the gas 1 respectively, and  $x_g$  and  $x_i$  (in mmol/mol) the values for total gas and individual gas contents given in Table 1. In Table 2 partial pressures thus obtained are given for total pipeline pressures of 10 bar ( $180^\circ$ ).

Again, the data can be divided into two groups, Wairakei with  $\log \text{P}_{\text{H}_2}$  and  $\log \text{P}_{\text{H}_2\text{S}}$  values of  $-4.5 \pm 0.1$  and  $-3.6 \pm 0.1$  respectively, and Kawerau and Broadlands with  $-3.7 \pm 0.7$  ( $\text{P}_{\text{H}_2}$ ) and  $-2.7 \pm 0.2$  ( $\text{P}_{\text{H}_2\text{S}}$ ). At present, the effects of geothermal steam corrosion have been studied in any detail only for Wairakei, this area is, therefore, discussed first.

TABLE 1

The chemical composition of steam carried in Wairakei steam lines or separated from Rawerau and Broadlands well discharges (in mmol/mol), together with sampling date, discharge enthalpies and steam separation temperatures, ST.

Date	E J/g	ST	x <sub>g</sub>	CO <sub>2</sub>	H <sub>2</sub> S	NH <sub>3</sub>	H <sub>2</sub>	N <sub>2</sub>	CH <sub>4</sub>
<b>Wairakei *</b>									
A 8.79	-	148°	.54	941	44.5	15.1	7.71	9.1	3.7
C 8.79	-	148°	.81	960	34.8	4.8	7.11	25.4	26
J 8.79	-	177°	.44	933	56.0	10.9	5.9	26.3	5.0
L 8.79	-	177°	.44	923	67.0	95	56	11.2	39
<b>Kawerau</b>									
K7 14. 2.78	1030	172°	7.6	951	38.8	3.73	0.52	1.65	41
K8 15. 2.78	1030	185°	9.3	932	27.9	3.87	1.77	9.58	24.6
K19 16. 2.78	1210	174°	7.3	916	38.2	4.75	2.82	11.70	26.1
<b>Broadlands</b>									
B11 29.10.76	1080	183°	12.6	955	16.4	3.98	1.42	6.80	15.9
B23 29.10.76	1325	154°	89	962	13.8	4.49	1.57	5.50	12.9
B25 29.10.76	1390	205°	19.5	947	11.2	1.82	2.39	11.75	26.1

\* Data for Wairakei steamlines were provided by R.B. Glover (pers. comm.)

TABLE 2

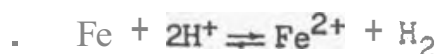
Logarithms of CO<sub>2</sub>, H<sub>2</sub>S and H<sub>2</sub> partial pressure in Wairakei, Kawerau, and Broadlands steam at 180°C together with calculated pH's of condensate in equilibrium with steam at 150° and 180°.

	Wairakei				Kawerau			Ohaki		
log P <sub>i</sub>	C	J	L		7	8	19	11	23	25
CO <sub>2</sub>	-2.29	-2.11	-2.30	-2.39	-1.14	-1.06	-1.18	-2.69	-1.07	-.73
H <sub>2</sub> S	-3.62	-3.55	-3.40	-3.53	-2.53	-2.59	-2.56	-2.69	-2.91	-2.66
H <sub>2</sub>	-4.38	-4.24	-4.59	-4.61	-4.40	-3.78	-3.07	-3.75	-3.70	-3.33
pH <sub>150°</sub>	6.79	6.56	6.70	6.66	6.52	6.55	6.58	6.56	6.59	6.40
pH <sub>180°</sub>	6.59	6.37	6.50	6.47	6.34	6.36	6.40	6.38	6.41	6.22

## Wairakei Steam Line Corrosion

At Wairakei two types of steam are produced: high pressure steam at a pressure close to 10 bar (180°) and carried in J- and L-line, and intermediate pressure steam at around 5 bar (150°) carried in the other lines. Severe corrosion has been reported for the high-pressure J- and L-lines. In Figure 2 the chemical processes likely to occur during the passage of steam through the pipeline in terms of the coordinates  $P_{H_2}$  and  $R = \log Fe^{2+}/(H^+)^2$  are given for these two operating pressures. At the very low hydrogen sulfide pressures observed at Wairakei, the mineral system to be considered consists largely of the oxide phases, pyrrhotite is unlikely to form at all, while pyrite occupies only a limited area.

Condensate forming from the steam entering the pipeline is initially very low in iron, on contact with the pipeline, iron dissolves and local evolution of hydrogen leads to an increase in  $P_{H_2}$  roughly in proportion to the amount of iron dissolved. The upper limit of  $P_{H_2}$  is given by the total pressure in the pipeline. Dissolution of iron according to



also leads to the consumption of hydrogen ions and the addition of  $Fe^{2+}$  and therefore to a rapid increase in

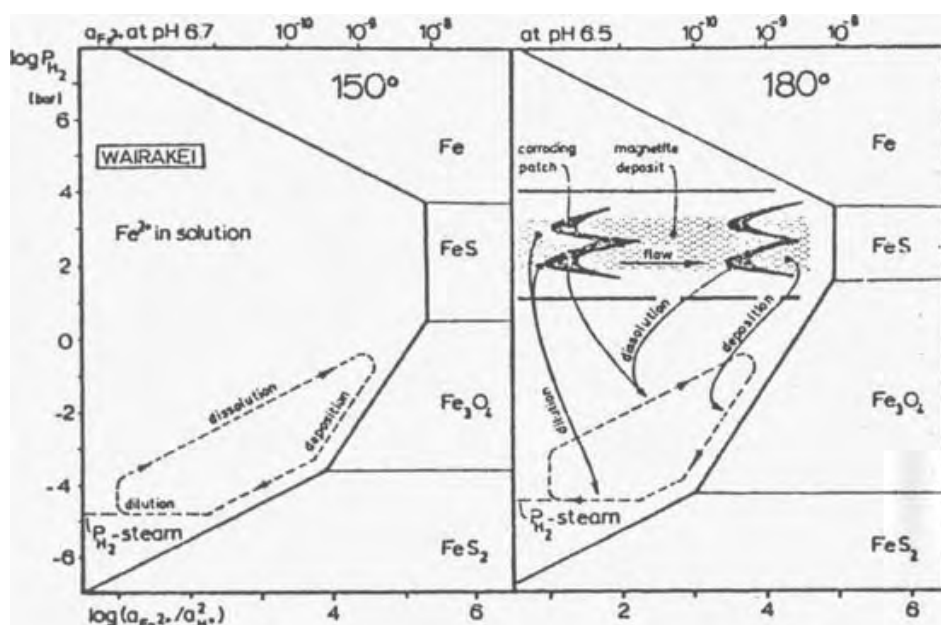


Figure 2 - The stability of iron minerals in contact with Wairakei production steam at 150° and 180°. Dashed lines delineate cyclic corrosion and magnetite deposition process.

$R = \log(\text{Fe}^{2+}/(\text{H}^+)^2)$  and the condensate composition moves along the Fe-dissolution line of Figure 2. At values of  $R$  of around 4 it enters the magnetite stability field. Subsequent deposition of magnetite accompanied by the release of protons moves the chemical system within the condensate along the magnetite deposition line to a point where, at least theoretically, some pyrite should be formed. Minor amounts of pyrite have been found interspersed in the magnetite layers (Braithwaite 1979) supporting that reaction sequence. Further deposition of iron in the form of pyrite or magnetite brings the chemical system within a drop of condensate to a position reflecting thermodynamic equilibrium of the iron scale deposited with the steam moving through the pipeline.

This state of equilibrium, however, is soon disturbed by the formation of additional, fresh condensate over the pipe line wall, reducing the iron concentrations in the drop. In Figure 2, this process is represented by the line marked 'dilution'. Movement of the system into the  $\text{Fe}^{2+}$  stability field implies undersaturation of the system with respect to any mineral to the right and therefore a tendency for the dissolution of any deposit that may have formed earlier. In the Wairakei pipeline this process is reflected in the destruction of the magnetite layer, reducing it to an easily detached, sometimes powdery, substance. Once the magnetite scale is sufficiently weakened, the liquid making up our drop is able to penetrate through to the underlying iron surface. The increase in  $\text{PH}_2$  associated with the ensuing corrosive attack moves our drop upwards further into the  $\text{Fe}^{2+}$  stability field of Figure 2 to a position corresponding to even greater undersaturation with respect to the secondary iron minerals to the right. Attack on the pipeline can be expected to be quite vigorous before saturation with respect to magnetite is again achieved.

The cyclic nature of these processes is reflected in the regular distribution of corrosion patches and products. Downstream of one of the drain pots, at intervals removing condensate from the pipeline, the corrosion patches are small and closely spaced ( $\sim 0.3$  m), with increasing distance and volume of condensate formed, these patches become larger and more widely spaced (1.50 m). This behaviour can be explained in terms of increased iron dissolution and deposition capacity of the volume of condensate increasing with distance. The above reaction scheme is also able to explain the often observed M shape of the corrosion patches. Fluid flow over these M's is always from top to bottom, the two angles pointing towards the preferred path of fresh condensate moving down from the pipeline walls. Incomplete mixing gives rise to accumulation of fresh condensate at the margin of the flow and therefore to increased corrosion there. The corrosion patches gradually move upstream with the arms of the top part of an M forming the leading edge. Once the condensate is saturated with respect to magnetite, deposition of this mineral occurs rapidly downstream in the form of the black crystalline deposits with individual crystals reaching a size of 3 mm.

Assuming full attainment over these Fe-dissolution and redeposition cycles, the amounts of iron involved may be estimated by use of

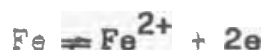
$$\log m_{\text{Fe}^{2+}} \approx \log a_{\text{Fe}^{2+}} = R - 2\text{pH}$$

Because of the very small amounts of iron involved, the pH of the condensate can be expected to remain unaffected by these processes and close to that resulting from the absorption of  $\text{CO}_2$ ,  $\text{H}_2\text{S}$  and  $\text{NH}_3$  from the vapour phase. In Table 2 calculated values of pH for pipeline temperatures of  $150^\circ$  and  $180^\circ$  are given. In spite of considerable variations in steam composition, the values obtained are quite uniform for all systems, around 6.6 at  $150^\circ$  and 6.4 at  $180^\circ$ . In Figure 2 values for  $m_{\text{Fe}^{2+}}$  calculated by use of the above equation are shown. Magnetite deposition then takes place over a concentration range from around  $10^{-9}\text{m}$  ( $-0.06\text{ mg/kg}$ ) to  $10^{-10}\text{m}$ ; pyrite deposition is restricted to even lower concentration ranges explaining the small amounts of pyrite found in the scale deposit.

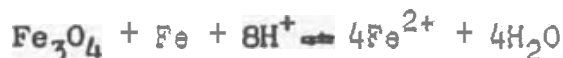
Electrolytic effects are likely to play an important part in the mechanisms affecting the stability of the magnetite scale (Braithwaite, 1979). In close electrolytic contact the dissolution of magnetite



may be coupled to the iron dissolution reaction



through direct transfer of electrons from the iron surface to the disintegrating magnetite scale. Because of the strong dependence of the overall reaction



on  $R = \log \text{Fe}^{2+}/(\text{H}^+)^2$ , this mechanism can only become active once pH and  $\text{Fe}^{2+}$  have dropped to a level allowing the system to overcome electrochemical barriers e.g. associated with irreversible processes on the iron and magnetite electrodes. The process giving rise to the reduction in pH and  $\text{Fe}^{2+}$  is dilution by the fresh condensate caused by heat loss from the pipelines. It is the continuous formation of fresh condensate which keeps the cyclic corrosion processes going.

The overall processes described above apply also to the low pressure (5 bar) pipelines. Because of the shift of the magnetite-pyrite transition point from  $R=3$  to  $R=4$ , implying formation of pyrite from more highly concentrated solutions, the proportions of pyrite in the scales formed at  $150^\circ$  can be expected to be somewhat higher as compared to one formed at  $180^\circ$ .



### Steam Line Corrosion Expected for Broadlands and Kawerau

At present no information on the type and degree of corrosion of pipelines carrying steam from Broadlands or Kawerau is available. Because of the good agreement between observed and theoretical corrosion behaviour observed for Wairakei steam, an attempt is made to delineate corrosion processes expected for Broadlands and Kawerau steam.

The main difference between Broadlands-Kawerau and Wairakei steam is the generally higher gas content. The higher absolute  $H_2S$  contents cause pyrite and pyrrhotite stability fields to expand (Figure 3) to completely replace magnetite as a stable phase. On contact with exposed iron the condensate composition can be expected to move along the iron dissolution line until the pyrrhotite boundary is reached. Deposition of a pyrrhotite film prevents further iron condensate interaction allowing the condensate to equilibrate with the vapor phase. The subsequent reduction in  $P_{H_2}$  is not accompanied by any additional mineral deposition until the pyrite stability boundary is reached. From then onwards most of the excess iron in solution is deposited in the form of pyrite until again a position corresponding to equilibrium among vapor, liquid and scale deposit is reached. As at Wairakei, addition of fresh condensate can then be expected to lead to undersaturation with respect to the scale deposit formed earlier, completing the cycle.

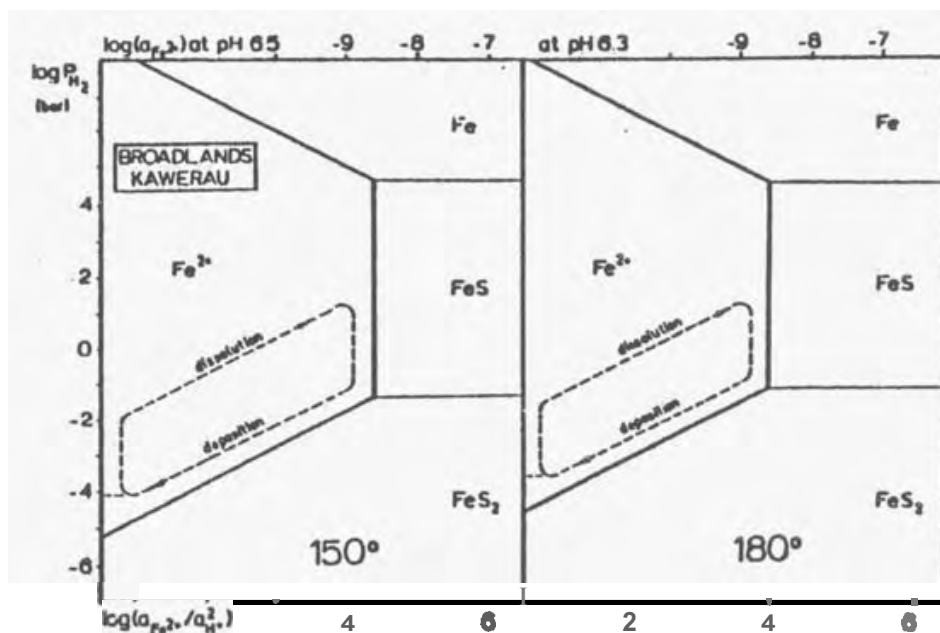
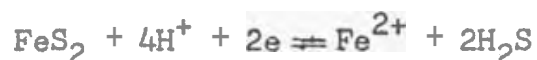


Figure 3 - Stability of Iron species in contact with Broadlands and Kawerau steam at 150° and 180°.

Because of the lower dissolved iron concentrations involved, the degree of corrosive attack on the pipeline is likely to be less severe than that at Wairakei, also the different nature of the scale deposit (pyrite) may have a pronounced effect on the stability of the protecting layers. Based on the reaction



electrolytic processes similar to those involved for the destruction of the magnetite scale can be expected to affect the stability of the pyrite deposit. A much more stable situation would result if for some reason pyrrhotite would be the main scale forming mineral. Because of its vertical boundary towards the  $\text{Fe}^{2+}$  stability field, no large variations in R would result from either the deposition or dissolution of FeS and the whole system would be quite independent of  $\text{P}_{\text{H}_2}$  conditions, conducive to the formation of a stable scale deposit. At present, however, no information is available to relate these theoretical behaviour patterns to those actually occurring.

#### Possible Strategies to Control Corrosion in Steam Lines

Accepting the above suggestion that the main reason for cyclic corrosion observed at Wairakei is the continuous formation of fresh condensate, one way to reduce corrosive attack would be to reduce the rate of condensate formation. Removal of condensate by increasing the number of drain pots is likely to simply increase the frequency of corroding patches without affecting the overall degree of corrosion. On the other hand, removal of the drain pots can be expected to lead to the establishment of few, but large and widely spaced corrosion patches. A technique to completely preclude condensate formation was recently proposed by James (1979). He suggests the creation of a pressure drop over the length of the pipeline sufficient to maintain the steam in a slightly superheated state and therefore to prevent the formation of condensate due to unavoidable heat loss. The economic effects of this reduction in operating pressure, or conversely flow rate, will have to be balanced against those of corrosion.

A possible chemical alternative (James, 1979) resulting from the application of the above mineral phase diagrams to the corrosion problem is represented by Figure 4. Here the stability fields of fayalite, ferrosilite and an iron-aluminium silicate for silica contents of 600 mg/kg are shown. The position of the boundaries for minerals actually forming under pipeline conditions is somewhat uncertain due to the lack of reliable thermodynamic data on the stability of hydrated

iron-silicates. The line designated Fe-Al-silicate corresponds to the stability of an iron rich chlorite in equilibrium with the geothermal liquid. The position of this boundary suggests extremely low equilibrium  $\text{Fe}^{2+}$  concentrations of below  $10^{-11} \text{ m}$  ( $< 1 \mu\text{g/kg}$ ) and therefore very small quantities of iron involved in corrosion processes associated with the formation of such an iron-aluminium silicate. Another important feature is the vertical boundary to the  $\text{Fe}^{2+}$  stability field. As with pyrrhotite, the existence of such a vertical boundary more or less prevents the establishment of the cyclic corrosion process described for minerals whose formation is dependent on hydrogen partial pressure, such as magnetite or pyrite. In the case of a vertical boundary the amount of iron dissolved is likely to correspond only to the low and uniform concentrations required to maintain a thin film of scale mineral in accordance with its solubility. In the case of  $P_{\text{H}_2}$  dependent deposits, equilibrium  $\text{Fe}^{2+}$  concentrations may fluctuate widely giving rise to large degrees of under- or supersaturation and therefore to the dissolution and deposition of large amounts of metallic iron or iron scale respectively, far beyond the amounts required to maintain a coherent protective layer.

The formation of a coherent Fe-silicate scale may explain the absence of magnetite-corrosion over the up-field parts of Wairakei pipelines. There, carryover of a spray of silica supersaturated thermal waters from the cyclone separators may provide the chemical environment for the formation of such a deposit. Further downstream removal of condensate through drain pots also removes any silica carried over in the spray

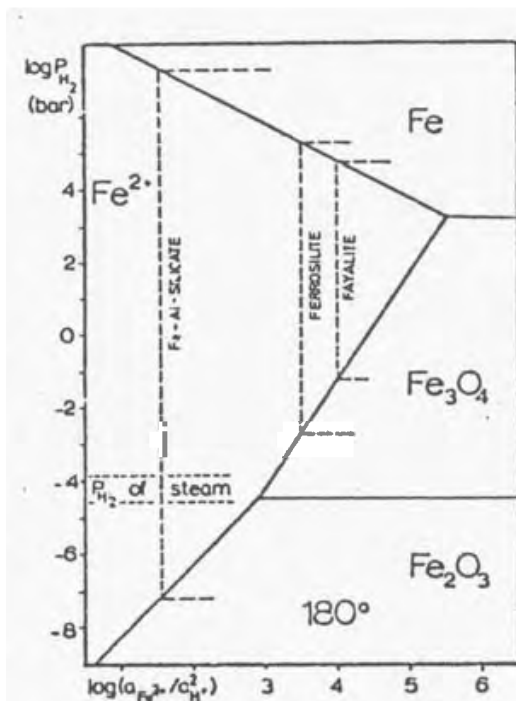


Figure 4 - Stability of iron silicates in contact with geothermal steam at 180°. Silica and aluminium concentrations in the Condensate are those of the deep thermal water.

- and corrosion as described above sets in. A possible way to control corrosion, therefore, would be to constantly replenish silica (and alumina) contents by the injection of thermal waters at intervals into the pipelines. The formation of coherent iron-silicate scale could possibly also be induced by "painting" the inside of the pipes with a thin slurry of cement during shut-down periods. The excess of cement likely to remain on the pipeline walls after such treatment should provide a sufficient reservoir to supply freshly forming condensate for a long time with the aluminium and silica required to maintain a stable iron-aluminium-silicate scale. A similar reservoir could be provided by replacing short sections of steel pipe by pipes lined with a suitably formulated concrete.

#### ACKNOWLEDGMENT

The author is grateful to Mr W.R. Braithwaite, Chemistry Division, DSIR for many helpful discussions and his Introduction to the subject of geothermal corrosion at Wairakei. The present study is materially based on his work on Wairakei steam line corrosion.

#### REFERENCES

1. Braithwaite, WR (1979) Corrosion in the 30 inch steam pipelines at the Wairakei geothermal field. (Unpublished manuscript).
2. Helgeson, H.C., Delany, J.M., Nesbitt, H.W., and Bird, D.K. (1978) Summary and critique of the thermodynamic properties of rock-forming minerals. *Am. J. Science* 278A, 1-229.
3. James, R (1979) Suppression of steam condensate corrosion at Wairakei geothermal power project (in press) .
4. Page, G.G. (1978) Corrosion in the 30 inch steam lines at Wairakei geothermal field. Field inspection 17 to 19th January 1978. Unpublished DSIR Report.
5. Pound, BG, Sharp, RM, and Wright, G.A. (1979) Geothermal Corrosion, Part 2, Electrochemical phase diagrams for Iron in geothermal media. University of Auckland, Unpublished Report.
6. Pourbaix, MJN. (1949) Thermodynamics of dilute aqueous solutions, London, Arnold,